

Integratable 40 dB optical waveguide isolators using a resonant-layer effect with mode coupling

Jacob M. Hammer

Photonics Consulting, Annapolis, Maryland 2140

Gokhan Ozgur, Gary A. Evans,^{a)} and Jerome K. Butler

Department of Electrical Engineering, Southern Methodist University, Dallas, Texas 75275-0338

(Received 13 July 2006; accepted 22 August 2006; published online 28 November 2006)

Resonant-layer effect (RLE) optical isolators can be integrated with a wide variety of optical waveguide devices and systems and theoretically provide a high degree of isolation with low insertion loss. The effect of mode coupling within the isolator and the losses due to coupling between the isolator and the input and output waveguides on the performance of RLE isolators is calculated. The results predict that isolators integrated with semiconductor waveguides similar to those used for efficient lasers and amplifiers and isolators integrated with quartzlike waveguides can give 40 dB of isolation with insertion losses below 3 dB. The calculations also show relaxed dimensional tolerance and lengths in the 1–2 mm range, which makes commercial production of such isolators attractive. © 2006 American Institute of Physics. [DOI: 10.1063/1.2388040]

I. INTRODUCTION

There is a widespread need for optical isolators in fiber optics and free space optical communication and in other applications of lasers and amplifiers. Large-scale integration of photonic components requires integrated isolators. Although a number of integrated waveguide isolators have been reported in the literature,^{1–17} optical isolators used in communications and in other systems have to date all been bulk devices. A review of the effect of mode coupling on the operation of resonant-layer-effect (RLE) isolators⁷ is given in this paper. These isolators can be integrated with a wide variety of optical waveguide devices and systems and promise a high degree of isolation with low insertion loss. The analysis includes coupling losses into and out of the isolator and shows that isolators integrated with semiconductor waveguides similar to those used for efficient lasers and amplifiers can give more than 40 dB of isolation with insertion loss below 3 dB. Isolators integrated with quartzlike waveguides also give more than 40 dB of isolation with losses below 3 dB. These results do not require tight dimensional and material tolerances, suggesting high yield in commercial production of such isolators.

The RLE isolators rely on adding a layer containing a ferromagnetic composite to an optical waveguide in the presence of a bias magnetic field. The added layer is called the resonant layer (RL). The waveguide, including the added layer, may have two principal modes. The guide mode has its maximum intensity in the guide layers and the second mode (RL mode) has its maximum intensity in the RL. The thickness (t_r) and position of the RL are chosen so that in one direction of propagation the guide and RL modes are very near phase match. In this case the guide mode has a large secondary field peak in the RL resulting in high insertion loss. In the opposite direction the nonreciprocal, magneto-

optic Faraday/Kerr effect substantially changes the index of the RL so that the phase match condition is no longer met, resulting in a small secondary peak and low insertion loss. This phenomenon is referred to as the resonant-layer effect. The real part of the effective index N_g of the guide mode will be close to that of the RL mode, N_r , when the modes are phase matched. In this work a RLE semiconductor isolator identical to that described by Hammer *et al.*⁷ is treated in addition to two quartz-based isolators.

Both the phase match condition and the resulting increase in the field overlap were achieved via correct choice of the thickness and relative position of the coupled waveguides in Ref. 7. Neither the effect of coupling between the guide and RL modes nor that of loss due to input and output waveguides was, however, considered. These effects are now treated here. An adaptation of an approximate numerical, coupled mode method that includes loss is used. This method is described in detail by Hammer *et al.*¹⁴ and is outlined in the Appendix.

In the magneto-optic Kerr effect, the complex refractive index depends on the direction and magnitude of a bias magnetic field and the direction of light propagation. This effect has been used to form waveguide isolators as described by a number of authors.^{1,2,4} None of these approaches makes use of the benefit available by working near a phase matched condition between the guide mode and the RL mode.

The isolation and insertion loss of a semiconductor–multi-quantum-well (MQW) isolator identical to the one treated here were calculated in Ref. 7. The nominal isolation is ≈ 328 dB/cm and the insertion loss is ≈ 14 dB/cm. The length for a device with 30 dB of isolation would be $910 \mu\text{m}$ if mode coupling were neglected. The results are, however, applicable only to a device of length sufficiently small that the effect of coupling between the guide and RL modes can be ignored. As will be shown below, the critical coupling length L_{crit} is $\approx 21 \mu\text{m}$ in the isolation direction, $H(-)$, and $121 \mu\text{m}$ in the forward, $H(+)$, direction. In a distance short

^{a)}Electronic mail: gae@enr.smu.edu

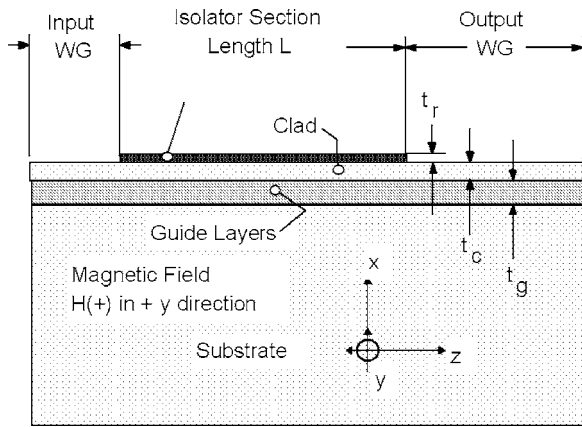


FIG. 1. Schematic diagram of an isolator based on RLE including input and output waveguide sections. Light propagates in the z direction.

enough to neglect mode coupling, e.g., $L_{\text{crit}}/5$, the isolation would be 0.14 dB. It is thus essential to include the effect of mode coupling to evaluate the RLE isolators.

It is also important to provide means of coupling light into and out of the isolator section to realize a key advantage to this type of isolator, which is that it can be integrated with other guided wave devices. Waveguides for this purpose are included in the analysis and shown in Fig. 1, which is a general schematic for the isolators discussed in this paper.

The z - y planar-optical waveguide, illustrated in Fig. 1, consists of a substrate of refractive index n_s , a guide layer (or layers) of index n_g and thickness t_g , and a clad (cover) layer of index n_c and thickness t_c . A composite layer of thickness t_r that consists of a host material containing nanometer-sized ferromagnetic particles, such as iron, is deposited on the clad in the isolator section. This layer is called the resonant layer and exhibits the magneto-optic Kerr effect in the presence of a bias magnetic field with a component parallel to the magnetic component of the optical field. A bias magnetic field, $H(+)$, parallel to the y direction will interact with a TM-like waveguide mode traveling in the z direction. Reversing the bias magnetic field is equivalent to reversing the direction of the guided mode. $H(-)$ is used to denote the reversed case.

Input and output guides that retain the layers of the isolator section without the RL are placed as shown in Fig. 1. These are intended to provide relatively efficient coupling to and from the isolator. Evaluating isolator performance without including the effect of input and output couplings may lead to misleading performance predictions.

II. THEORY

The effective complex refractive indices, near fields and field overlap for both directions of propagation are calculated with the MODEIG (Ref. 18) waveguide computer program. These numbers are needed as the basis for all the calculations. The real part of the effective refractive index for the guide and RL modes is $N_g(\pm)$ and $N_r(\pm)$, respectively. The imaginary parts of the effective refractive index for the guide and RL modes are $k_g(\pm)$ and $k_r(\pm)$, respectively. The (+) sign refers to the forward direction, $H(+)$, and the (-) to the reverse direction, $H(-)$. The subscript g is used to label

TABLE I. Fe-semiconductor-composite resonant-layer (FSC-RL) layer structure isolator. The waveguide layers are similar to those of an InGaAsP-MQW-semiconductor laser.

$\lambda = 1.55 \mu\text{m}$ FSC-RL isolator			
Layer material	Layer loss α (cm^{-1})	Layer refractive index	Layer thickness (μm)
Air	0	1	...
RL $H(+)$ Fe-InGaAsP	229	3.4042	Optimum=0.414
RL $H(-)$ Fe-InGaAsP	336	3.3930	
p -clad InP	0	3.1628	Optimum=2.3
Barrier InGaAsP	0	3.37	0.05
Five QW InGaAsP	0	3.46	0.01
Four Barriers InGaAsP	0	3.37	0.01
Barrier GaInAsP	0	3.37	0.05
n -clad InP	0	3.1628	0.50
Substrate n -InP	0	3.1628	...

quantities associated with the guide mode, and the subscript r labels quantities associated with the RL mode.

The modal loss (gain) coefficient is

$$\alpha_i(\pm) = 2\pi k_i(\pm)/\lambda \quad (i = r, g). \quad (1a)$$

Positive values of k or α indicate loss. Note that in the MODEIG program the term NLOSS is identical to α in units of $1/\mu\text{m}$. The power loss in dB/cm is

$$20 \log[\exp(-\alpha_i(\pm) \times 10^4)] \quad \text{for } \lambda \text{ in } \mu\text{m} \quad (i = r, g). \quad (1b)$$

In the forward direction, $H(+)$, the power loss is the insertion loss and in the backward direction, $H(-)$, it is the isolation. The coupling coefficient between guide and RL modes is

$$\kappa_{g,r}(\pm) = UC_{g,r}(\pm). \quad (2)$$

$C_{g,r}$ is the normalized field amplitude overlap between the guide mode and the RL mode that may be obtained from the "overlap" program in MODEIG and

$$U = 2 \frac{\sqrt{(n_g^2 - N_g^2)(N_g^2 - n_c^2)}}{N_g \lambda}. \quad (3)$$

Here n_g is the average index of the guide layers and n_c is the index of the cladding. This relation is semiempirical and based on the expression for $\kappa_{g,r}$ given by Ref. 19.

Please note that in the cases considered, $C_{g,r} = C_{r,g}$ and $\kappa_{g,r} = \kappa_{r,g}$. Thus, we define $\kappa_{g,r} \kappa_{r,g} = |\kappa_g|^2$. For complex $C_{g,r}$, both real and imaginary parts are multiplied by U and the squares added to get $|\kappa_g|^2$. These constants are used to calculate the effect of the coupling between the guide and RL modes as detailed in the Appendix.

The coupling amplitude from input or output waveguide (WG) to the guide mode is approximated by

$$A_g(\pm) = \frac{\sqrt{K(\pm)_{gw}}}{\sqrt{K(\pm)_{rw}} + \sqrt{K(\pm)_{gw}}}. \quad (4a)$$

The coupling amplitude from input or output WG to the RL mode is approximated by

TABLE II. Complex effective indices, loss coefficients, coupling coefficients, and the critical coupling length L_{crit} for the FSC-RL isolator.

	N_g	N_r	k_g	k_r	$\alpha_g/\mu\text{m}$	$\alpha_r/\mu\text{m}$	$ \kappa_g ^2$	$\kappa/\mu\text{m}$	$L_{\text{crit}} = \pi/\kappa$ (μm)
$H(+)$	3.190 51	3.1964	4.08×10^{-5}	1.39×10^{-3}	1.653×10^{-4}	5.630×10^{-3}	1.0659×10^{-4}	2.6001×10^{-2}	120.8
$H(-)$	3.190 50	3.1909	9.31×10^{-4}	1.05×10^{-3}	3.775×10^{-3}	4.271×10^{-3}	1.4733×10^{-2}	1.2134×10^{-1}	25.9

$$A_r(\pm) = \frac{\sqrt{K(\pm)_{rw}}}{\sqrt{K(\pm)_{rw} + \sqrt{K(\pm)_{gw}}}}. \quad (4b)$$

$K(\pm)_{gw}$ is the normalized intensity overlap between the guide mode and the mode of the input/output waveguide. $K(\pm)_{rw}$ is the normalized intensity overlap between the RL mode and the mode of the input/output waveguide. These are also obtained from the overlap program in MODEIG.

III. IRON-SEMICONDUCTOR-COMPOSITE RESONANT-LAYER ISOLATOR

The layers of a semiconductor-based isolator are shown in Table I. The stack of five quantum wells (QWs) is separated by barriers to form the guide layers. This device will be referred to as the Fe-semiconductor-composite, resonant-layer (FSC-RL) isolator.

The RL consists of nanometer-sized iron particles with a volume fill fraction $q=0.02$ in an InGaAsP host. The loss reduction factor is assumed to be $1/30$.^{20,21} The method used to calculate the loss and index of the composite is described in Ref. 7. The optimum p -clad and RL thicknesses are shown in Table I. As mentioned earlier, excluding coupling effects, a nominal isolation of 328 dB/cm and an insertion loss of 14.4 dB/cm are calculated from Eq. (1b). Substantial isolation and low loss are predicted for practical isolator lengths when the effects of mode and input-output coupling are included as will be seen in Sec. IV.

Values obtained for the constants used in the mode coupling calculation for the FSC-RL isolator are listed in Table II. As can be seen, the critical coupling length L_{crit} in the forward direction, $H(+)$, is about $120 \mu\text{m}$ and in the reflected or isolator direction, $H(-)$, it is less than $26 \mu\text{m}$. This, as pointed out earlier, makes it essential to consider the coupled mode solutions to evaluate isolator operation. Note that κ is found using Eqs. (A4) and (A5) from the Appendix. The input amplitudes to the isolator section are taken in the $H(+)$ direction, and are calculated to be $A_g(+)=0.993$ and

$A_r(+)=0.113$. It is assumed that the input light excites the lowest order guide mode of the input waveguide at unity intensity. The light reflected back at the isolator corresponding to the $H(-)$ direction is also assumed to excite the lowest order guide mode of the output guide with unity intensity. In this direction the input amplitudes to the isolator section are $A_g(-)=0.984$ and $A_r(-)=0.178$. The input coupling loss is included in the coupled mode formalism. The output coupling loss is given by $20 \log[A_g(+)] = -0.056$ dB. Fresnel reflection is negligible because the real parts of the effective indices of all the modes differ only in the third decimal place.

IV. RESULTS OF THE COUPLING CALCULATIONS FOR THE FSC-RL ISOLATOR

Figures 2 and 3 are plots of the isolation and insertion loss as a function of isolator length for the FSC-RL isolator. Figure 2 is a detailed plot in the vicinity of $z \approx 12 \mu\text{m}$, about half a critical coupling length in the $H(-)$ direction. The isolation is more than 20 dB for $10.7 < L < 12.3 \mu\text{m}$ and more than 30 dB for $11.3 < L < 11.7 \mu\text{m}$. The insertion loss for these cases is below 0.24 dB. Clearly, attempting to obtain 30 dB of isolation by working at such short lengths requires a very high tolerance of $\approx \pm 0.2 \mu\text{m}$. A short 20 dB device would require a length tolerance of $\approx \pm 1.6 \mu\text{m}$ that is clearly difficult, especially if the tolerances on the compositions and layer thicknesses are also considered.

Figure 3 shows the behavior over a longer length. For lengths around $850 \mu\text{m}$ the minimum isolation is 30 dB. As the length is increased above $800 \mu\text{m}$, isolation will vary above 30 dB to values greater than 50 dB with a period of $\approx 26 \mu\text{m}$, which is the $H(-)$ critical coupling length. The isolation will be greater than 40 dB for lengths greater than $\approx 1100 \mu\text{m}$. The insertion loss is below 2.4 dB in the 30 dB isolation range and less than 2.9 dB in the 40 dB isolation range. Thus, with a relaxed tolerance on length, a device

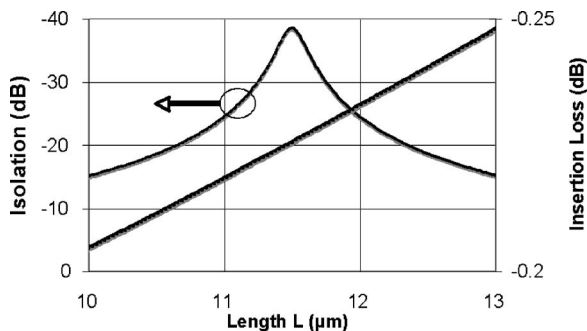


FIG. 2. FSC-RL isolator. Isolation and insertion loss as a function of isolator section length L between 10 and $13 \mu\text{m}$.

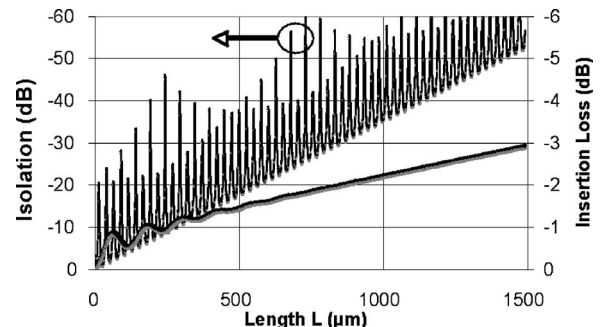


FIG. 3. FSC-RL isolator. Isolation and insertion loss as a function of isolator section length L between 0 and $1500 \mu\text{m}$. Please note that at this length scale the peak (largest negative) values of isolation are not resolved.

TABLE III. Fe-polymer-composite resonant-layer (FPC-RL) isolator with fill fraction (a) $q=0.02$ and (b) $q=0.1$.

Layer material	Loss α (cm^{-1})	Real part of refractive index	Optimum thickness (μm)
(a) $\lambda=1.55 \mu\text{m}$, FPC-RL isolator; fill fraction $q=0.02$			
Air	0.0	1.0000	...
RL $H(+)$ Fe-polymer composite	44.15	1.5678	$t_r=2.0$
RL $H(-)$ Fe-polymer composite	83.37	1.5630	
Cover (clad), quartz	0.0	1.447	$t_c=4.5$
Guide Layer, doped quartz	0.0	1.452	$t_g=7.4$
Substrate quartz	0.0	1.447	...
(b) $\lambda=1.55 \mu\text{m}$, FPC-RL isolator; fill fraction $q=0.1$			
Air	0.0	1.0000	...
RL $H(+)$ Fe-polymer composite	227.5	1.6812	$t_r=0.452$
RL $H(-)$ Fe-polymer composite	426.9	1.6562	
Cover (clad), quartz	0.0	1.447	$t_c=3.4$
Guide layer, doped quartz	0.0	1.452	$t_g=7.0$
Substrate quartz	0.0	1.447	...

with reliable isolation of at least 40 dB and insertion loss less than 3 dB can be obtained using lengths around 1200 μm .

V. IRON-POLYMER-COMPOSITE RESONANT-LAYER ON QUARTZ ISOLATORS

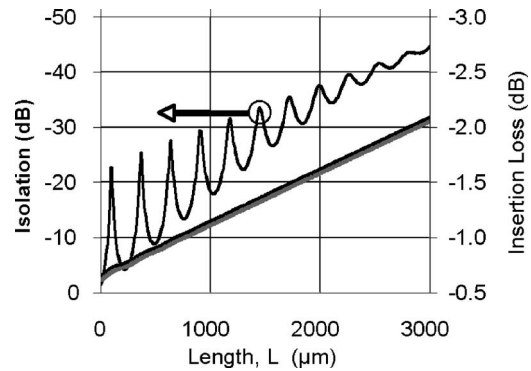
In this section isolators using composite RLs based on nanometer-sized particles of iron in a polymer host^{20,21} will be treated. Specifically, a perfluorocyclobutyl polymer with $n=1.54$ (Ref. 22) deposited on quartz-based waveguides are considered. These devices will be referred to as Fe-polymer-composite resonant-layer (FPC-RL) isolators. The layers are shown in Tables III(a) and III(b).

Two different fill factors $q=0.02$ and $q=0.1$ for the RL will be considered. A ferromagnetic polymer composite with a fill factor $q=0.02$ has been reported.²¹ A composite with a fill factor as large as 0.1 is more speculative and was included to see what, if any, advantage would be realized by using larger fill factor composites. The input and output sections retain the layers of the isolator section without the RL.

The optimum RL, p -clad, and guide layer thicknesses for the $q=0.02$ case are shown in Table III(a). A nominal isolation of 74 dB/cm and an insertion loss of 4.7 dB/cm are calculated from Eq. (1b) excluding the effect of coupling. The values for the $q=0.1$ case are shown in Table III(b).

TABLE IV. Complex-effective indexes, loss coefficients, coupling coefficients, and the critical coupling length L_{crit} for the FPC-RL isolator with (a) $q=0.02$ and (b) $q=0.1$.

	N_g	N_r	k_g	k_r	$\alpha_g/\mu\text{m}$	$\alpha_r/\mu\text{m}$	κ_g^2	$\kappa/\mu\text{m}$	$L_{\text{crit}}=\pi/\kappa$ (μm)
(a) $q=0.02$									
$H(+)$	1.450 4	1.4531	1.33×10^{-5}	5.78×10^{-4}	5.406×10^{-5}	2.341×10^{-3}	8.5470×10^{-7}	1.1069×10^{-2}	283.8
$H(-)$	1.450 4	1.450 8	2.10×10^{-4}	7.52×10^{-4}	8.504×10^{-4}	3.047×10^{-3}	1.3336×10^{-4}	1.1591×10^{-2}	271.0
(b) $q=0.1$									
$H(+)$	1.450 2	1.455 4	3.20×10^{-5}	1.25×10^{-3}	1.298×10^{-4}	5.084×10^{-3}	2.1443×10^{-7}	2.1250×10^{-2}	147.8
$H(-)$	1.450 2	1.450 5	6.90×10^{-4}	9.50×10^{-4}	2.795×10^{-3}	3.850×10^{-3}	3.6496×10^{-5}	6.1338×10^{-3}	512.2

FIG. 4. FPC-RL isolator with $q=0.02$. Isolation and insertion loss as a function of isolator section length L between 0 and 3000 μm .

Here, again excluding coupling, a nominal isolation of 243 dB/cm and an insertion loss of 11.3 dB/cm are calculated. Substantial isolation and relatively low insertion loss with practical isolator lengths are predicted for both cases when the effects of coupling between the guide mode and RL mode and that of input and output couplings are included.

Values obtained for the constants used in the mode coupling calculation for the FPC-RL isolator are listed in Tables IV(a) and IV(b). It is again assumed that the input and the reflected light excite the lowest order mode of the input and output waveguides at unity intensity, respectively. For the $q=0.02$ case, the input amplitudes to the isolator section are $A_g(+)=0.952$ and $A_r(+)=0.307$ in the $H(+)$ direction. In the $H(-)$ direction the amplitudes are $A_g(-)=0.842$ and $A_r(-)=0.539$. The output coupling loss is -0.214 dB.

For the $q=0.1$ case, the amplitudes are $A_g(+)=0.973$, $A_r(+)=0.233$, $A_g(-)=0.744$, and $A_r(-)=0.668$. The output coupling loss is -0.241 dB.

VI. RESULTS OF THE COUPLING CALCULATIONS FOR THE FPC-RL ISOLATORS

Figures 4 and 5 are plots of the isolation and insertion loss as a function of isolator length for the FPC-RL isolators. In the $q=0.02$ case shown in Fig. 4, for 30 dB isolation the isolator section would be above 1650 μm long and have less than 1.3 dB insertion loss with a large tolerance on the length. To a higher tolerance, 30 dB of isolation would be obtained for L in the range of 1410–1490 μm with loss less than 1.2 dB. For a 40 dB isolator, the length would be over 2500 μm with insertion loss of less than 2.1 dB.

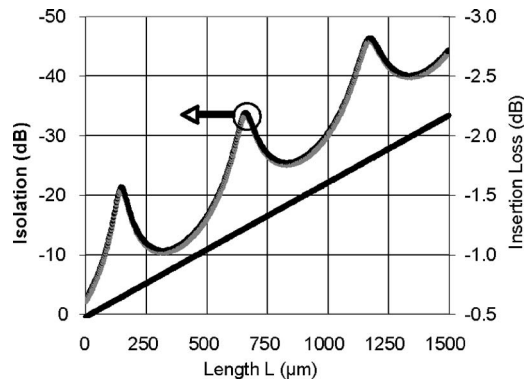


FIG. 5. FPC-RL isolator with $q=0.1$. Isolation and insertion loss as a function of isolator section length L between 0 and 500 μm .

In the $q=0.1$ case shown in Fig. 5, a 30 dB isolator could have an isolator section between 630 and 700 μm long with less than 1.3 dB insertion loss. To a lower tolerance, 30 dB of isolation would be obtained for L between 990 and 1100 μm with loss less than 1.8 dB. A 40 dB section would be longer than 1100 μm with insertion loss less than 2.0 dB. Thus, the FPC-RL isolator section with $q=0.1$ would be about half the length of the $q=0.02$ isolator but have similar performance. The shorter device is attractive, but the question remains open as to whether or not a composite with so large a fill factor can be realized.

VII. CONCLUSION

The effect of mode coupling on the operation of resonant-layer effect (RLE) isolators⁷ that can be integrated with a wide variety of optical waveguide devices and systems has been presented. The calculations show that isolators on semiconductor waveguides similar to those used for efficient lasers and amplifiers can give over 30 dB of isolation with insertion loss below 2.5 dB. Isolation of over 40 dB can be realized with insertion loss less than 3.0 dB. Isolators on quartzlike waveguides with more than 30 dB of isolation have insertion loss below 1.7 dB and isolation greater than 40 dB with insertion loss below 1.8 dB. The RLE isolators do not require high tolerance for practical lengths of 1000–2000 μm (1–2 mm range), which should be attractive for commercial production and application in a variety of integrated-optic systems.

APPENDIX: NUMERICAL METHOD USED FOR CALCULATION OF COUPLING BETWEEN GUIDE AND RL MODES

In the numerical calculation, G is the amplitude, P_g the intensity of the guide mode, R the amplitude, and P_r the intensity of the RL mode. The subscript g refers to the guide mode and r to the RL mode. In each case considered, both guide and RL modes have the same polarization (both TE or both TM).

The numerical calculation includes phase mismatch in addition to gain and/or loss and can accommodate unequal coupling coefficients. A computer spreadsheet such as Microsoft Excel is used and the elements are arranged in col-

umns. The rows (cells) of the first column (A) are used for the constants. Column B is the z distance with increment dz . Thus,

$$z_j = z_{j-1} + dz. \quad (\text{A1})$$

The subscript j refers to the row. The calculation assumes that there is only one guide mode and one RL mode that need to be considered. The guide mode amplitude G_j and RL field mode amplitude R_j at each incremental step dz are related as follows:

$$G_j = (1 - \alpha_g dz)G_{j-1} + \kappa dz R_j \quad (\text{in column C}), \quad (\text{A2})$$

$$R_j = (1 - \alpha_r dz)R_{j-1} - \kappa dz G_j \quad (\text{in column D}). \quad (\text{A3})$$

The effective coupling coefficient κ is given by

$$\kappa = \sqrt{\kappa_g^2 + \delta^2}, \quad (\text{A4})$$

where δ is the phase mismatch and is given by

$$\delta = 2\pi|N_g - N_r|/\lambda. \quad (\text{A5})$$

A factor Δ is defined as

$$\Delta = \sqrt{\kappa_g^2/\kappa}. \quad (\text{A6})$$

In order to obtain proper normalization and include phase mismatch, the field amplitudes that correspond to the normal modes without coupling, called g_j (for the guide mode) and r_j (for the RL mode), are calculated in separate columns. Thus, in column G for the guide mode,

$$g_j = (1 - \alpha_g dz)g_{j-1}, \quad (\text{A7})$$

and in column H for the RL mode,

$$r_j = (1 - \alpha_r dz)r_{j-1}. \quad (\text{A8})$$

The optical mode power (intensity) is now given by P_g in column E (guide mode intensity) and P_r in column F (RL mode intensity) where

$$P_g = (\Delta)(G_j)^2 + (1 - \Delta^2)g_j^2 \quad (\text{A9})$$

and

$$P_r = (\Delta)(R_j)^2 + (1 - \Delta^2)r_j^2. \quad (\text{A10})$$

In the absence of gain or loss the sum $P_g + P_r$ is constant in z as required by energy conservation. In addition, this numerical method gives the same results as the conventional coupled mode or simple propagation theory at the limits of (a) exact phase match without gain or loss, (b) phase mismatch without gain or loss, and (c) zero coupling with gain or loss. Thompson²³ gives a closed form theory for the case of weak coupling.

¹Y. Okamura, T. Negate, and S. Yamamoto, *Appl. Opt.* **23**, 1866 (1984).

²T. Mizumoto, K. Oochi, T. Harada, and Y. Naito, *J. Lightwave Technol.* **4**, 347 (1986).

³J. M. Hammer, J. H. Abeles, and D. J. Channin, *IEEE Photonics Technol. Lett.* **9**, 631 (1997).

⁴W. Zaets and K. Ando, *IEEE Photonics Technol. Lett.* **11**, 1012 (1999).

⁵M. Levy, *IEEE J. Sel. Top. Quantum Electron.* **8**, 1300 (2002).

⁶V. Zayets, M. C. Debnath, and K. Ando, *Appl. Phys. Lett.* **84**, 565 (2004).

⁷J. M. Hammer, G. A. Evans, G. Ozgur, and J. K. Butler, *J. Lightwave Technol.* **22**, 1754 (2004).

⁸M. Vanwolleghem *et al.*, *Appl. Phys. Lett.* **85**, 3980 (2004).

- ⁹J. J. Wang, J. Deng, X. Deng, F. Liu, P. J. Sciortino, L. Chen, A. Nikolov, and A. Graham, *IEEE J. Sel. Top. Quantum Electron.* **11**, 241 (2005).
- ¹⁰V. Zayet and K. Ando, *Appl. Phys. Lett.* **86**, 261105 (2005).
- ¹¹S. Bhandare, S. K. Ibrahim, D. Sandel, H. Zhang, F. Wüst, and R. Noé, *IEEE J. Sel. Top. Quantum Electron.* **11**, 417 (2005).
- ¹²M. Greenberg and M. Orenstein, *IEEE J. Quantum Electron.* **41**, 1013 (2005).
- ¹³N. Kono and M. Koshiba, *IEEE Photonics Technol. Lett.* **17**, 1432 (2005).
- ¹⁴J. M. Hammer, J. H. Abeles, and D. J. Channin, SBIR Contract No. DASG60-95-C-0070, Final Report, 31 January 1996.
- ¹⁵H. Shimizu and Y. Nakano, *J. Lightwave Technol.* **24**, 38 (2006).
- ¹⁶T. Mizumoto, OFC, TuE5, , Los Angeles, CA, 2004.
- ¹⁷M. Vanwolleghem *et al.*, OFC, TuE6, Los Angeles, CA, 2004.
- ¹⁸G. A. Evans, MODEIG/98, Version 6.0, Southern Methodist University, 1998. Available on-line at <http://www.seas.smu.edu/modeig/>. A revised version of the software is available at <http://enr.smu.edu/ee/smuphotonics/Modeig.htm>.
- ¹⁹S. Somekh, E. Garmire, A. Yariv, H. L. Garvin, and R. G. Hunsperger, *Appl. Phys. Lett.* **22**, 46 (1973).
- ²⁰K. Baba, F. Takase, and M. Miyagi, *Electron. Lett.* **32**, 222 (1996).
- ²¹K. Baba, F. Takase, and M. Miyagi, *Opt. Commun.* **139**, 35 (1997).
- ²²J. Ballato, S. Foulger, and D. W. Smith Jr., *J. Opt. Soc. Am. B* **20**, 1838 (2003).
- ²³G. H. B. Thompson, *J. Lightwave Technol.* **LT-4**, 1678 (1986).